Available online at www.sciencedirect.com
ScienceDirect
International Journal of Heat and Mass Transfer 50 (2007) 2024–2036
International Journal of HEAT and MASS TRANSFER
www.elsevier.com/locate/ijhmt

Technical Note

Experimental investigation on transfer characteristics of temperature fluctuation from liquid sodium to wall in parallel triple-jet

Nobuyuki Kimura *, Hiroyuki Miyakoshi, Hideki Kamide

Japan Atomic Energy Agency, 4002 Narita, O-arai, Ibaraki 311-1393, Japan

Received 26 July 2006; received in revised form 29 September 2006
Available online 5 December 2006

Abstract

A quantitative evaluation on thermal striping, in which temperature fluctuation due to convective mixing causes thermal fatigue in structural components, is of importance for integrity of nuclear reactors and also general plants. Sodium cooled fast reactor had also several incidents of coolant leakage due to the high cycle thermal fatigue. A sodium experiment of parallel triple-jet configuration was performed to evaluate transfer characteristics of temperature fluctuation from fluid to structure. The non-stationary heat transfer characteristics could be represented by a heat transfer coefficient, which was constant in time and independent of the frequency of temperature fluctuation.

Keywords: Sodium cooled fast reactor; Temperature fluctuation; Thermal striping; Heat transfer; Transfer function

1. Introduction

In nuclear reactors and general plants, temperature fluctuation occurs in the region where hot and cold fluids are mixed. The temperature fluctuation may cause structural components high cycle thermal fatigue, i.e., thermal striping. In fast reactors, liquid metal sodium is used as the coolant and it has the high thermal conductivity. The thermal striping as a phenomenological problem in liquid metal cooled fast reactors was already recognized in the early 1980s by Wood [1], Brunings [2] and has subsequently been studied by Betts et al. [3], Moriya et al. [4], Muramatsu [5] and Tokuhiro et al. [6]. The structural failures due to the high cycle thermal fatigue have occurred not only in the liquid metal cooled fast reactors but also in light water reactors and various general plants (Japanese PWR Tomari-2 in 2003, French PWR CIVAUX in 1998, and so on).

The thermal striping phenomena could be divided into five processes; (1) occurrence of temperature fluctuation due to the convective mixing between hot and cold fluids, (2) attenuation of temperature fluctuation in the boundary layer near the structure, (3) heat transfer from the fluid to the structure, (4) thermal conduction in structure and (5) thermal fatigue in structure. As for thermal hydraulic behavior in the thermal striping phenomena, Tenchine et al. [7,8] investigated the mixing of co-axial jets of sodium and compared the results of sodium with those of air. Tokuhiro et al. [9,10] and Kimura et al. [11,12] have performed a water experiment in parallel triple-jet and evaluated the mixing process among the jets. Igarashi et al. [13,14] has carried out a water experiment with T-pipe configuration and classified flow regimes into three flow patterns dependent on the momentum ratio of the inlet velocities between the main and branch pipes. As for the numerical investigation, Muramatsu [15] has developed numerical methods to evaluate thermal hydraulics and heat transfer from fluid to structure. As for studies on the structure, Wu and Janne Carlsson [16] evaluated the

* Corresponding author. Tel.: +81 29 267 4141; fax: +81 29 266 3867.
E-mail address: kimura.nobuyuki@jaea.go.jp (N. Kimura).

0017-9310/$ - see front matter © 2006 Elsevier Ltd. All rights reserved.
doi:10.1016/j.ijheatmasstransfer.2006.09.030

Nomenclature

A	amplitude of temperature fluctuation
a	thermal diffusivity
Bi	Biot number
D	representative length
D_e	hydraulic diameter
F	Fourier transform of temperature fluctuation
f	frequency of temperature fluctuation
H	transfer function
h	heat transfer coefficient
N	number of experimental data
Nu	Nusselt number
P	power spectrum density
Re	Reynolds number
T	temperature
T^*_{avg}	normalized time-averaged temperature
T^*_{RMS}	normalized temperature fluctuation intensity (root-mean-square of temperature fluctuation)
t	time
V	discharged velocity
x	horizontal axis along the structural wall
y	axis normal to the structural wall
z	vertical axis along the structural wall
ΔT	temperature difference
ε	phase
φ	phase of temperature fluctuation
λ	thermal conductivity
ω	angular velocity
ξ	distance between two positions

Subscripts

c	cold jet
f	fluid
h	hot jet
w	wall

distribution of the thermal stress in a structural plate and Kasahara et al. [17,18] developed the structural response diagram dependent on the frequency of temperature fluctuation in the fluid on the assumption of connection between fluid and structure via a heat transfer coefficient, which is constant in time. When the transfer of temperature fluctuation from fluid to structure is evaluated, it is of importance to determine the heat transfer coefficient. When the wall is insulated at the boundary except for one boundary where the temperature fluctuation is transferred, the time-averaged heat flux at the wall surface is nearly equal to zero. Therefore, the heat transfer coefficient can not be obtained from the time-averaged heat flux. Choe and Kwong [19] predicted the wall temperature using a convolution integral of fluid temperature. In Choe's study, the heat transfer coefficient was adequately given by the trial-and-error method.

In order to estimate the thermal striping, the processes (2)–(4) are significant on the point of the attenuation of temperature fluctuations. The quantitative evaluation of the attenuation makes it possible to design the legitimate structure in the plants with its integrity. However, there are few studies, which use liquid metal as a working fluid. In addition, it is needed to acquire the heat transfer coefficient deterministically.

In this study, we performed a sodium experiment in the triple-parallel jets along a stainless steel wall. The triple jets were configured as a cold jet in the center and hot jets in both sides. This geometry corresponds to a simplified two dimensional configuration of reactor core outlet which has cold flow channels of control rods surrounded with hot channels of fuel subassemblies. The authors have already carried out the water experiment of the triple-parallel jets [11,12]. Then the velocity and temperature fields were well understood in the triple jets. For the transfer of temperature fluctuation from fluid to structure, we developed how to acquire the time-constant heat transfer coefficient deterministically and we verified that the heat transfer coefficient was appropriate for the thermal stress.

2. Experiment

2.1. Experimental apparatus

Fig. 1 shows the schematic of the test section and thermocouples arrangement in a thermocouple-tree and a test plate. Each of the discharged nozzles had a shape of rectangular 20 mm × 180 mm. The height of the nozzles from the bottom was 85 mm and the both sides of the nozzle blocks had slopes. Three porous plates and the quadrant reducer nozzle were set upstream of the each nozzle. Fig. 2 shows the time-averaged velocity distribution at 0.1 mm from the nozzle exit obtained from the water experiment with the same nozzle geometry as the sodium experiment. The spatial-averaged velocity at the nozzle was 0.5 m/s. The local velocity was measured by the particle image velocimetry [20]. The velocity distribution at the nozzle exit showed the flat profile overall. Therefore, we made an assumption that the discharged velocity profile at the nozzle outlet could be flat in the sodium experiment. The cold jet flowed out vertically in the center and the hot jets flowed out in both sides of the cold jet. The nozzles and mixing region were sandwiched by the two vertical plates. Thus, three jets flow along the walls and the temperature fluctuation in the fluid is transferred to the plates. As for the coordinates, x-axis is horizontal direction along the wall surface, y-axis is normal direction

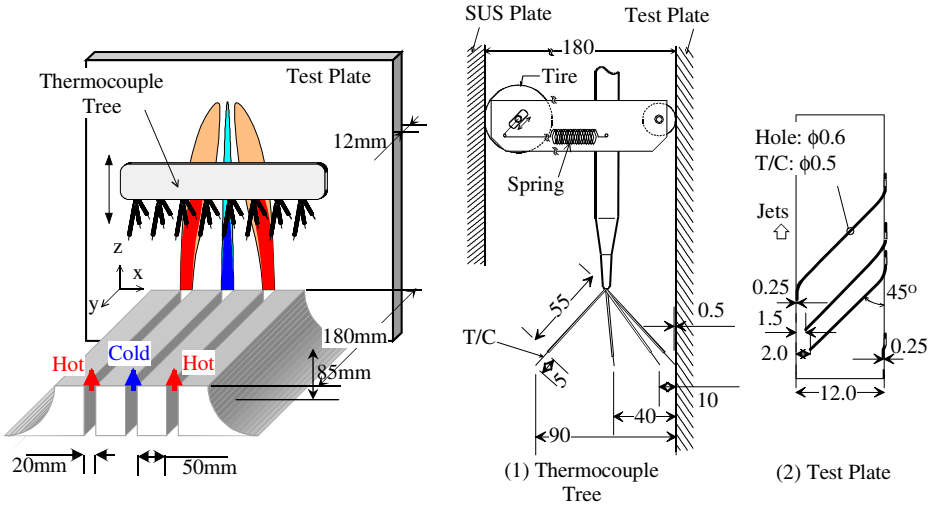

Fig. 1. Schematic of test section and thermocouple arrangement.

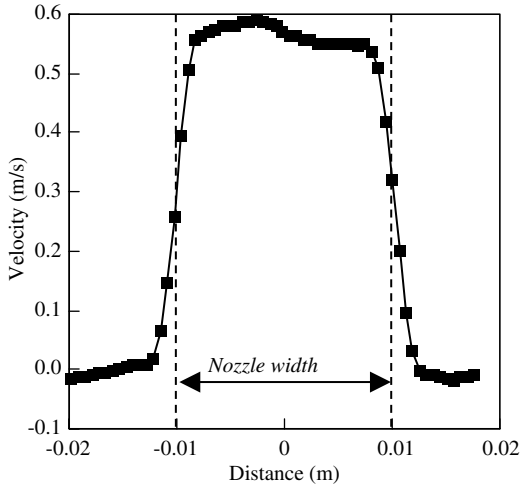

Fig. 2. Horizontal distribution of velocity at nozzle exit obtained from water experiment.

to the wall surface and z-axis is vertical direction along the wall surface. The position of the origin is the center of the cold jet in horizontally, the height of the nozzle exit vertically and on the wall in normal direction to the wall. The both plates were made of stainless steel type-316 (JIS SUS316) and thermocouples were buried in one plate, which is called a test plate. Temperature in the fluid was measured by a movable thermocouple-tree. The thermocouple-tree consisted of four arrays those had different distances from the wall surface. The each array had 25 thermocouples. The distances between the thermocouple-arrays and the wall surface were 90 mm, 40 mm, 10 mm and 0.5 mm within ±0.1 mm accuracy. To keep the distance from the wall surface constant, a moving tire with a spring pressed the thermocouple-tree against the opposite wall. For the target test plate, the fixed tire kept the distance constant between the thermocouple-arrays and the wall surface. The distances between thermocouples and the wall surface were confirmed in a mock-up test. The thermocouples in the test plate were inserted in the holes which were inclined by 45° to the wall surface to avoid an influence of thermocouple sleeve on the heat conduction in the wall. The thickness of the test plate was 12 mm. The measured points in the test plate were 0.25 mm, 1.5 mm, 2.0 mm and 11.75 mm from the wall surface facing the jets. The thermal contact positions in the thermocouples were confirmed by using X-ray examination. The thermocouples in the tree and test plate were non-contact K-type (chromel – alumel) and the diameter of thermocouple was 0.5 mm.

2.2. Experimental parameters

Table 1 shows the experimental conditions. The test cases were categorized in two conditions; the discharged velocity of the cold jet was the same as that of hot jets (isovelocity condition, case 1–9) and the velocity of cold jet was smaller than that of hot jets (non-isovelocity condition, case 10–13). The water experiment showed oscillatory swing of the center jet under the isovelocity condition and not under the non-isovelocity condition. The oscillatory motion resulted in a prominent frequency component of temperature fluctuation. On the other hand, random temperature fluctuation without the prominent frequency was observed under the non-isovelocity condition. In these two different flow patterns, the transfer characteristics of temperature fluctuation from liquid sodium to the structure can be investigated. Moreover, the discharged velocities in the sodium experiment were varied from 0.2 m/s to 1.0 m/s in order to clarify the effect of frequency of temperature fluctuation, which is proportional to the discharged velocity, on the transfer characteristics of temperature fluctuation from liquid sodium to the structure. In all cases of the non-isovelocity condition, the discharged velocity of cold jet was smaller by factor of 0.67 than that of the hot jets. The discharged temper-

Table 1
Experimental conditions

Case name	Hot jet				Center jet (cold)				ΔT (°C)	V_c/V_h
	V_h (m/s)	Re_h ($\times 10^4$)	Pe_h ($\times 10^2$)	T_h (°C)	V_c (m/s)	Re_c ($\times 10^4$)	Pe_c ($\times 10^2$)	T_c (°C)		
Case 1	0.20	1.13	0.63	342.7	0.20	1.06	0.62	310.5	32.2	1.0
Case 2	0.30	1.68	0.93	350.1	0.30	1.55	0.91	310.0	39.9	1.0
Case 3	0.34	1.87	1.03	349.5	0.33	1.72	1.01	310.7	38.6	1.0
Case 4	0.38	2.15	1.18	351.6	0.38	1.94	1.15	306.2	45.2	1.0
Case 5	0.51	2.83	1.57	347.7	0.51	2.60	1.55	304.5	43.0	1.0
Case 6	0.57	3.15	1.74	349.9	0.56	2.89	1.71	307.5	42.7	1.0
Case 7	0.70	3.85	2.14	344.7	0.69	3.59	2.11	310.0	34.7	1.0
Case 8	0.82	4.51	2.51	344.3	0.81	4.22	2.48	309.5	34.8	1.0
Case 9	1.01	5.53	3.09	340.8	1.00	5.18	3.05	309.8	30.8	1.0
Case 10	0.30	1.70	0.94	352.4	0.20	1.04	0.61	311.0	41.3	0.65
Case 11	0.51	2.87	1.58	349.8	0.32	1.68	0.99	311.0	38.7	0.63
Case 12	0.81	4.45	2.49	340.8	0.54	2.79	1.64	309.8	31.0	0.66
Case 13	1.01	5.54	3.11	338.5	0.68	3.50	2.06	308.5	30.0	0.67

ature difference between the hot and cold jets was approximately 40 °C in all cases.

2.3. Experimental methods

The discharged velocity was calculated using the flow rate obtained from the electromagnetic flow meter (EMF) in each line of the nozzle. The original specification of each EMF was a maximum measurement range of 30 m^3/h within 5% full-scale accuracy. Furthermore, the factual accuracy of the EMFs were improved within 0.1 m^3/h through means of drop method calibration. This accuracy corresponded to the velocity within ±0.008 m/s at the nozzle exit. The temperatures in fluid were measured at several heights by the movable thermocouple-tree. At each position of the thermocouple-tree, temperatures in structure and fluid were measured simultaneously. The accuracy of thermocouple was within 0.1 °C, and the time-constant of thermocouple was approximately 20 ms. The thermocouples were calibrated by a relative method based on the reference thermocouple, in which the electromotive voltage was known. The time-interval of temperature measurement was 0.01 s and the number of the recorded temperature was 20,000 at each position.

3. Results and discussion

3.1. Flow pattern of mixing among jets

Fig. 3 shows the two-dimensional (x-z) contours of the time-averaged temperature fields at $y = 90$ mm (mid position between the two walls) and $y = 0.5$ mm from the wall under the isovelocity condition ($V_h = V_c = 0.5$ m/s and $V_h = V_c = 1.0$ m/s) and the non-isovelocity condition ($V_h = 0.5$ m/s, $V_c = 0.33$ m/s and $V_h = 1.0$ m/s, $V_c = 0.68$ m/s). The temperature and the temperature fluctuation intensity were normalized as follows:

$$T^* = \frac{T - T_c}{\Delta T} \tag{1}$$

$$T^*_{RMS} = \frac{1}{\Delta T}\sqrt{\frac{\sum_i^N (T_i - T_{avg})^2}{N}}, \tag{2}$$

where $\Delta T = T_h - T_c$.

The masked area corresponds to some non-functional thermocouples. In the cases of isovelocity and non-isovelocity, two hot jets flowed upward and inclined to the cold jet. In the case of non-isovelocity, the cold jet leaned toward the hot jet in one side. The temperature fluctuation intensity under the isovelocity condition was largest at the region where the hot jet met the cold jet. The area of high fluctuation intensity region became small at the neighborhood of the wall surface in the both cases. The contours of time-averaged temperature and fluctuation intensity in the higher discharged velocity case were similar to those in the lower discharged velocity case. It means that the time-averaged temperature field was independent of the discharged velocity in the range from $V_h = 0.5$ m/s to 1.0 m/s.

Fig. 4 shows the time-trends of temperatures at the position ($x = -15$ mm, $z = 100$ mm), where the largest fluctuation was registered under the isovelocity condition ($V_h = V_c = 0.5$ m/s) and the non-isovelocity condition ($V_h = 0.5$ m/s, $V_c = 0.33$ m/s). The instantaneous temperature was normalized by Eq. (1). The measured positions in depth direction were $y = 90$ mm (mid position between the two walls), $y = 0.5$ mm (closest position to the wall surface), $y = -0.25$ mm (in the structure) and $y = -1.5$ mm (in the structure). Under only the isovelocity condition, periodic temperature fluctuation was observed. This periodic fluctuation is consistent to the water experiment [20] mentioned in Section 2.2.

The amplitude of fluid temperature fluctuation in the figure decreased as the measured position was close to the wall surface. Furthermore, temperature fluctuation decayed particularly in the structural wall. Thus, it is required to take into account this decay for the stress evaluation. It was shown that the wave of temperature was slightly delayed when temperature fluctuation was transferred from the fluid to the structure. Under the non-isovelocity condition, the periodic temperature fluctuation was

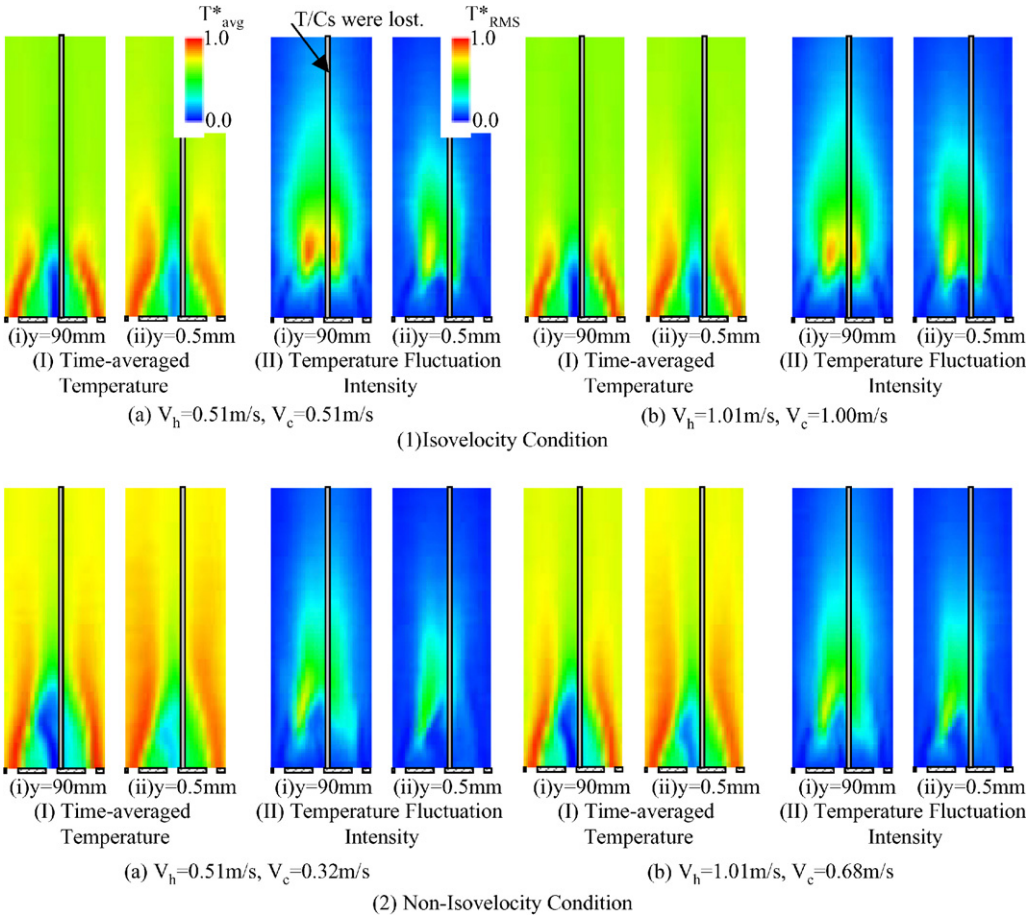

Fig. 3. Contours of time-averaged temperature fields.

not clear in comparison with that under the isovelocity condition.

Fig. 5 shows the power spectrum density (PSD) of temperature fluctuation at the same position as Fig. 3($x = -15$ mm, $z = 100$ mm) under the isovelocity ($V_h = V_c = 0.5$ m/s) and the non-isovelocity ($V_h = 0.5$ m/s, $V_c = 0.33$ m/s) conditions. In order to obtain the PSD, the temperature data set of 1024 ($=2^{10}$ and time length of 10.24 s) was extracted from total measured data (200 s) with a Gaussian window. Such the data sets were obtained 200 times so as to shift the data area by one second in the total measured data. The extracted data were converted to the data in frequency domain by the fast Fourier transform (FFT) and the PSD was obtained by averaging the total of 200 sets of FFT results. The prominent frequency component was observed in temperature fluctuation under the isovelocity condition as well as in the water experiment [20]. The PSDs in the fluid at $y = 90$ mm and $y = 0.5$ mm were nearly identical under the isovelocity condition. The PSDs under the non-isovelocity condition did not have a prominent frequency of temperature fluctuation. On the transfer process of the temperature fluctuation from the fluid ($y = 0.5$ mm) to the structure ($y = -0.25$ mm), the decay of the higher frequency component was larger than that of the lower frequency component in both cases.

3.2. Heat conduction characteristics in structure

An investigation on non-stationary behavior of heat conduction inside the structure is of importance in order to evaluate thermal stress in the structure caused by the random temperature fluctuation. The temperature history at the wall surface is required to obtain the heat flux at the wall surface and the heat transfer coefficient, and also to evaluate the thermal stress in the structure. The heat conduction analysis will help to obtain the temperature history and heat flux at the wall surface. The instantaneous heat transfer could be obtained from the predicted heat flux and the temperature difference between fluid and structural surface.

When temperature fluctuation is given as $A\sin(\omega t + \varphi)$ at one position ($\xi = 0$) of infinite plate, the theoretical equation of the one-dimensional non-stationary heat conduction for a single period wave at any point in the plate thickness direction, ξ, is as follows:

$$T(t,\xi) = A\exp\left(-\sqrt{\frac{\omega}{2a}}\xi\right)\sin\left(\omega t + \varphi - \sqrt{\frac{\omega}{2a}}\xi\right), \tag{3}$$

We made an assumption that the heat conduction process had linear characteristics for wave period or angular frequency, ω. It means that the heat conduction of the random temperature fluctuation in the structure is represented

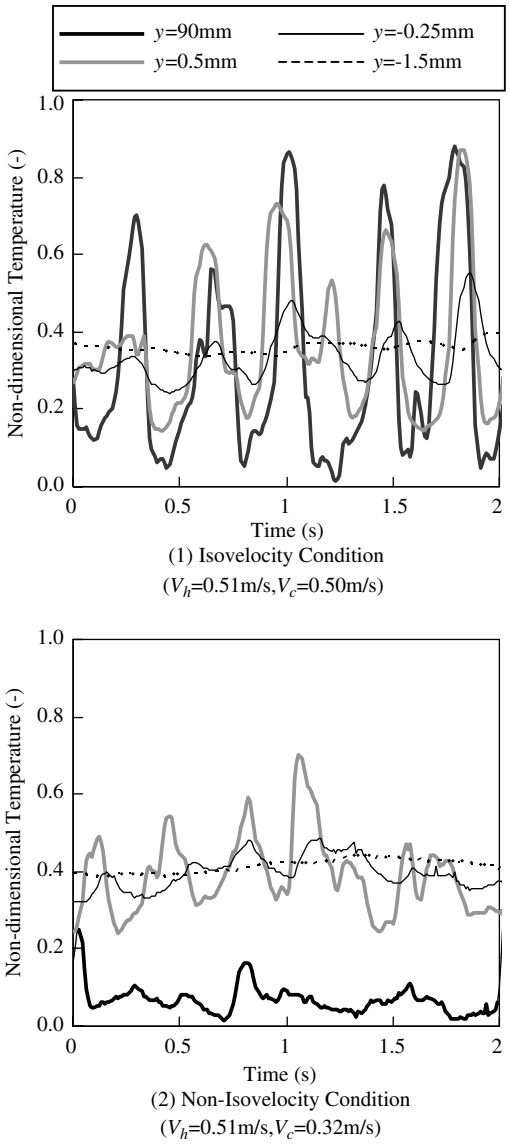

Fig. 4. Time-trends of temperatures at the position where the largest fluctuation was registered.

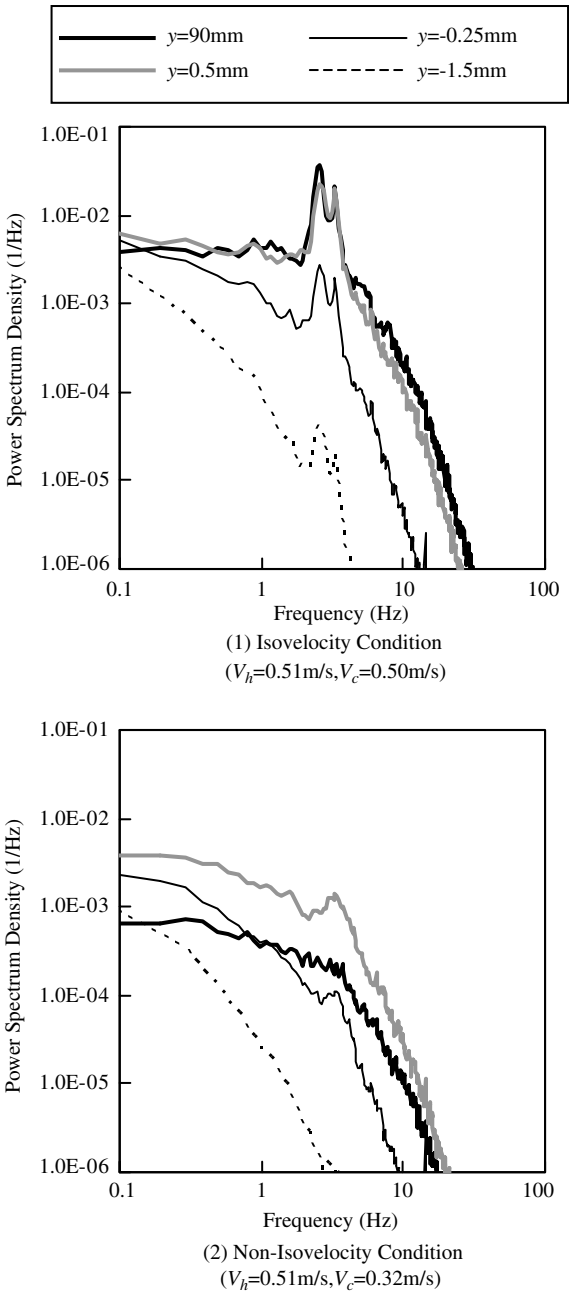

Fig. 5. Power spectrum density of temperature fluctuation.

as the linear combination of every frequency components. Then, a transfer function of temperature fluctuation between two positions (distance, ξ) will be represented as follows:

$$\begin{aligned}&\text{Amplitude}: \exp\left(-\sqrt{\frac{\omega}{2a}}\xi\right),\\ &\text{Phase delay}: \sqrt{\frac{\omega}{2a}}\xi\end{aligned} \tag{4}$$

In the sodium experiment, the transfer function between two points, $y = -0.25$ mm and $y = -1.5$ mm in the wall was obtained as follows:

$$H(f) = \frac{F_2(f)}{F_1(f)}, \tag{5}$$

where $H(f)$ is the transfer function. $F_1(f)$ and $F_2(f)$ were Fourier transforms of measured temperature histories, which obtained from the same method as the acquisition of the PSD.

Fig. 6 shows the power and the phase delay obtained from the transfer function in the experiments together with theoretical curves of Eq. (4). The horizontal axis is a frequency and the vertical axis is the power or the phase in the transfer function. The experimental results were in good agreements with the theoretical solution independent of the velocity conditions. It was confirmed that the conduction process of random temperature fluctuation in structure was predicted by a transfer function deduced from the well-known non-stationary one-dimensional thermal conduction equation.

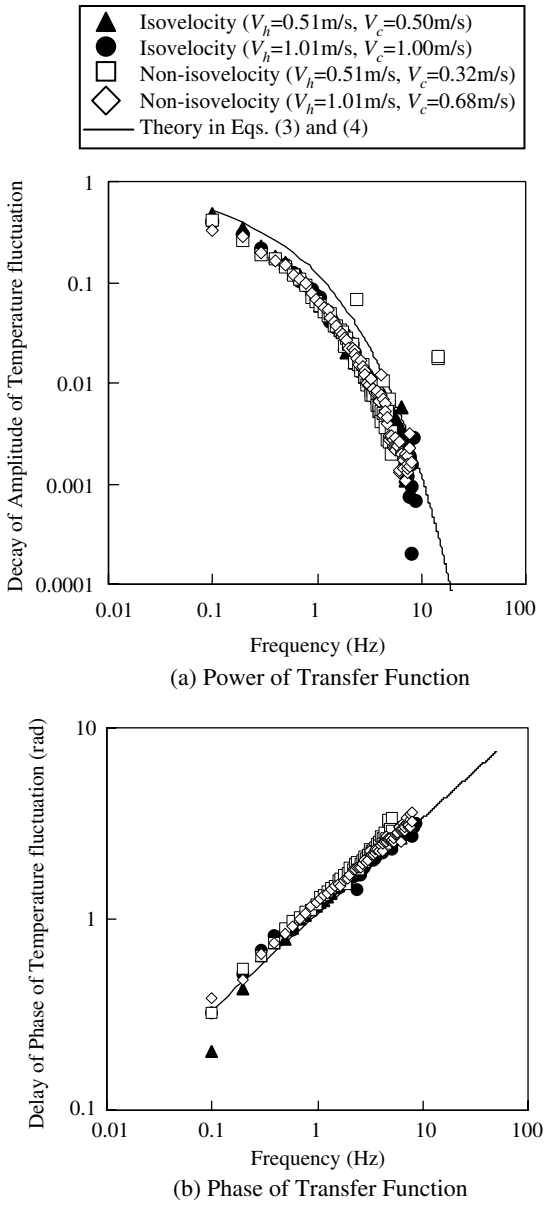

Fig. 6. Decay of the power and the delay of the phase in temperature fluctuations between the two points ($y = -0.25$ mm and $y = -1.5$ mm) in structure.

By using this transfer function, it will be possible to predict the temperature history and also the heat flux at the wall surface from the measured temperature data at a certain position in the wall. Before this, prediction of temperature history is demonstrated in Fig. 7. The temperature history at $y = -0.25$ mm was predicted from the measured temperature at $y = -1.5$ mm and compared with the measured data. The prediction method is as follows:

(1) Temperature history at $y = -1.5$ mm was converted in frequency domain by FFT,
(2) The transfer function of Eq. (4) was operated and frequency characteristics of power and phase at $y = -0.25$ mm were obtained,
(3) Temperature history was obtained by inverse FFT.

Here, frequency components of power and phase lower than 10 Hz were used in the processes (2) and (3) to eliminate the measurement error or noise in high frequency component in the measured temperature data at $y = -1.5$ mm. The predicted results at $y = -0.25$ mm were in good agreements with the measured data in all cases. Then, we considered that the temperature history at the wall surface can be predicted based on the temperature data at $y = -0.25$ mm.

For a single period wave, the instantaneous heat flux at the structural surface ($\xi = 0$ mm) was obtained from Eq. (3) as follows:

$$q(\omega) = \sqrt{2}A\lambda\sqrt{\frac{\omega}{2a}}\sin\left(\omega t + \varphi + \frac{\pi}{4}\right), \tag{6}$$

As discussed before, the conduction process in the wall is expressed by linear combination of frequency component. Thus the transfer function from the surface temperature (at $x = 0$) to the heat flux at $x = 0$ is as follow:

$$\begin{aligned} &\text{Power: } \left(\sqrt{2}\lambda\sqrt{\omega/2a}\right)^2. \\ &\text{Phase delay: } -\pi/4 \end{aligned} \tag{7}$$

Then it is possible to estimate the heat flux at the wall surface by the wall surface temperature based on the transfer function.

Fig. 8 shows the comparisons of time-trends between temperatures in fluid and structure and the heat flux at the wall surface. The fluid temperature was measured at $y = 0.5$ mm from the wall surface. The structural temperature at the wall surface was predicted by applying the transfer function of Eq. (4) to the temperature in the wall at $y = -0.25$ mm. Positive value of the heat flux means that the heat flows from the fluid to the structure. The heat flux largely fluctuated around zero and the time-averaged heat flux was nearly equal to zero. The fluid temperature near the wall surface, the temperature at the wall surface and the heat flux at the wall surface were obtained. Then, it is possible to acquire the instantaneous heat transfer coefficient. The heat transfer characteristics obtained from the heat flux was discussed in the next section.

3.3. Transfer characteristics of temperature fluctuation from fluid to structure

In order to evaluate the thermal stress in the structure, the instantaneous temperature distribution in the structure is needed. Especially, it is important to acquire the temperature distribution in thickness direction in the structure. The structural temperature at the neighborhood of the surface was represented by the non-stationary one-dimensional thermal conduction equation in Section 3.2. The heat transfer coefficient is required to get the surface temperature from the fluid temperature.

Fig. 9 shows the trends of the instantaneous heat transfer coefficient and the temperature difference between the

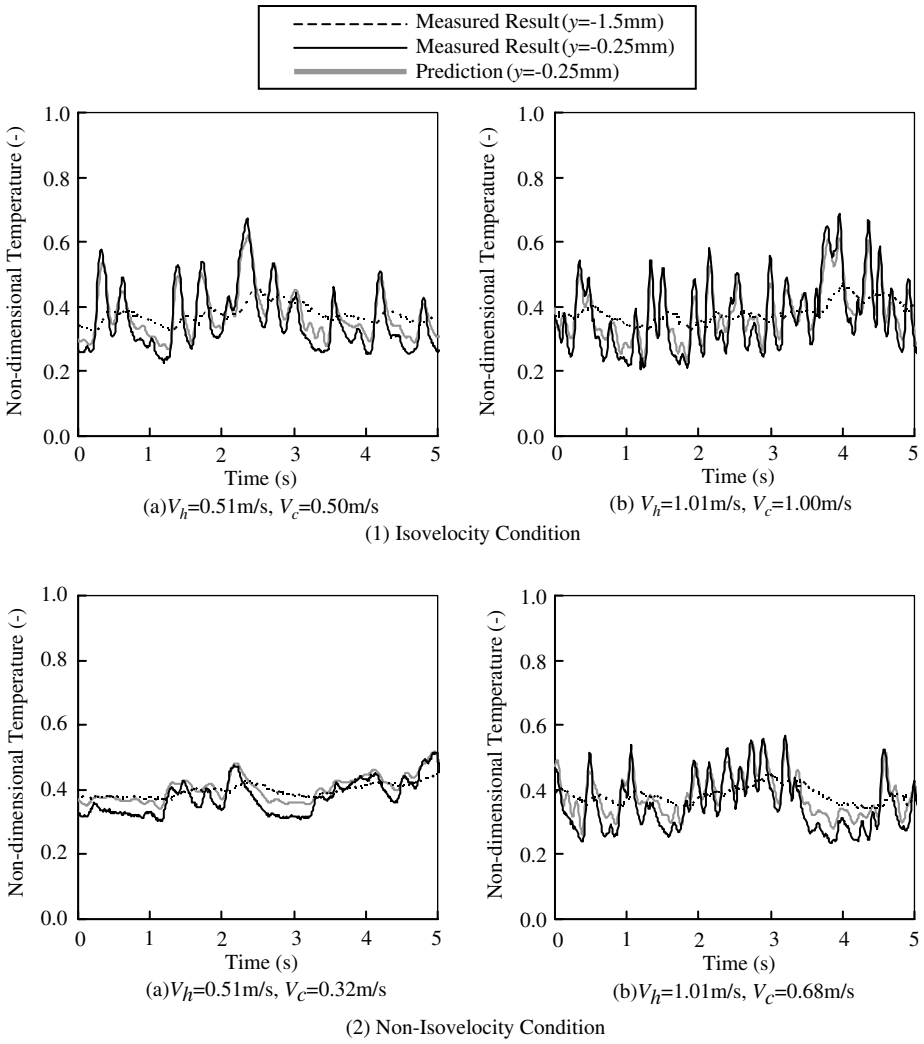

Fig. 7. Prediction of temperature fluctuation at the neighborhood of the structural surface ($y = -0.25$ mm) using the experimental results in the structure ($y = -1.5$ mm).

fluid ($y = 0.5$ mm) and the surface ($y = 0$ mm). The instantaneous heat transfer coefficient was defined as follows:

$$h = q/\Delta T. \tag{8}$$

Here, the instantaneous heat flux was calculated by using the measured temperature in the structure based on Eq. (6). The instantaneous temperature difference, ΔT, was defined as the difference between the fluid temperature at $y = 0.5$ mm and the structural temperature at the wall surface predicted by using the temperature at $y = -0.25$ mm. The heat transfer coefficient oscillated largely as well as the temperature at $y = 0.5$ mm. It was seen that the instantaneous heat transfer coefficient showed the local maximal value when the ΔT was close to zero. Due to the definition, the heat transfer coefficient will have large uncertainty when the ΔT is close to zero. Therefore it is expected that the instantaneous heat transfer coefficient does not have so large variation and fluctuated around a constant value.

Kasahara et al. [21] showed an evaluation method using Biot number based on a constant heat transfer coefficient in time to obtain the frequency response of the thermal stress in the structure. It is difficult to apply the heat transfer coefficient, which fluctuate temporally, to this evaluation method. In other words, the constant heat transfer coefficient in time is required to evaluate the thermal stress in the structure for a simple and easy design method.

The instantaneous heat transfer coefficient fluctuated as shown in Fig. 9. However, a constant heat transfer coefficient, h, is assumed for the simplicity. Then the transfer function is extended from the wall inside to the relation between the fluid and the wall by using the heat transfer coefficient, h.

First, the transfer functions were obtained from the experimental data to see the influence of flow velocity, namely amplitude of h. Fig. 10 shows the transfer functions of temperatures from the fluid ($y = 0.5$ mm) to the structure ($y = -0.25$ mm) under the isovelocity and non-isovelocity conditions. The transfer function was defined as Eq. (5). The power of the transfer function in the higher discharged velocity case was larger than that in the lower

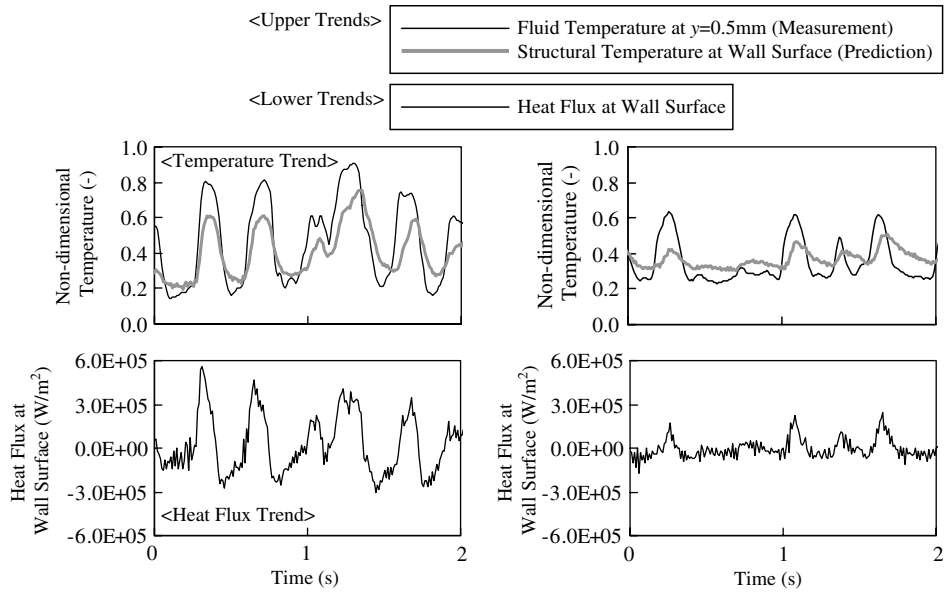

(1) Isovelocity Condition (V_h=0.51m/s, V_c=0.50m/s) (2) Non-Isovelocity Condition (V_h=0.51m/s, V_c=0.32m/s)

Fig. 8. Comparisons of trends between temperatures in fluid and structure and heat flux at wall surface.

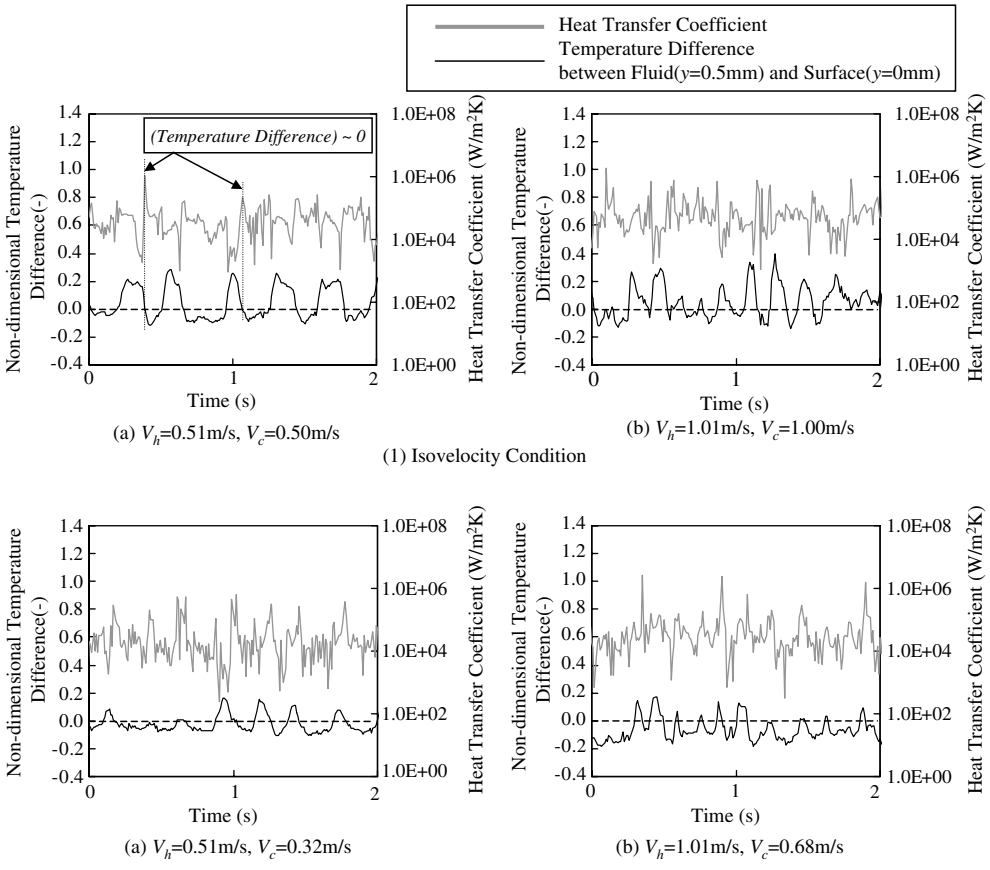

(a) V_h=0.51m/s, V_c=0.50m/s (b) V_h=1.01m/s, V_c=1.00m/s

(1) Isovelocity Condition

(a) V_h=0.51m/s, V_c=0.32m/s (b) V_h=1.01m/s, V_c=0.68m/s

(2) Non-Isovelocity Condition

Fig. 9. Trends of instantaneous heat transfer coefficient.

discharged velocity case under isovelocity and non-isovelocity conditions. This is due to the larger heat transfer coefficient in the higher velocity case. The phase in the transfer function in the higher velocity case was smaller than that in the lower discharged velocity case in overall frequency range. However, the data points of the phase showed scattered distribution. It would appear that one of the reasons for the scattered phase data is the small cor-

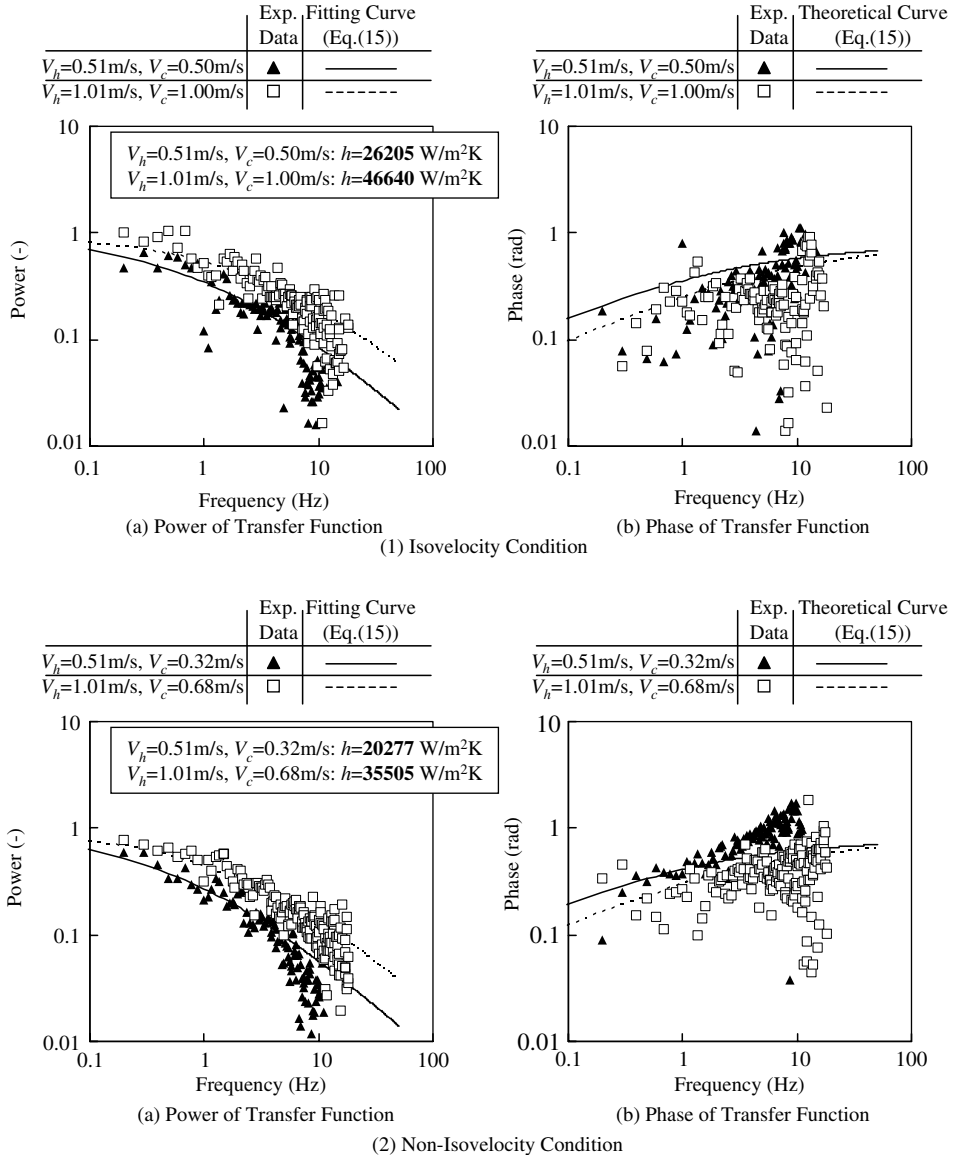

Fig. 10. Transfer function between the fluid to the structure under the isovelocity and non-isovelocity conditions.

relation due to the measurement error in high frequency component.

As shown in Fig. 10, the power of the transfer function will be correlated with the amplitude of the heat transfer. Next, the theoretical transfer function of temperature fluctuation from the fluid to the structure is deduced. In one-dimensional sense, the temperatures in fluid and wall are correlated as follows:

$$q(t) = h\{T_{\mathrm{f}}(t) - T_{\mathrm{w}}(t,0)\}, \tag{9}$$

$$q(t) = -\lambda \left.\frac{\partial T_{\mathrm{w}}(t,\xi)}{\partial \xi}\right|_{\xi=0}, \tag{10}$$

where $q(t)$ is heat flux at the wall surface, $T_{\mathrm{f}}(t)$ is fluid temperature, $T_{\mathrm{w}}(t,\xi)$ is structural temperature given as the functions of time, t, and distance from the wall surface, ξ. Here, h is assumed to be constant in time for the simplicity as mentioned before.

In addition, the non-stationary one-dimensional heat conduction equation, in which a semi-infinite plate is assumed, is as follows:

$$\frac{\partial T_{\mathrm{w}}(t,\xi)}{\partial t} = a\frac{\partial^2 T_{\mathrm{w}}(t,\xi)}{\partial \xi^2}. \tag{11}$$

When fluid temperature fluctuates according to the equation of $T_{\mathrm{f}}(t) = A\sin(\omega t + \varphi)$, the temperature in the wall, $T_{\mathrm{w}}(t,\xi)$, is acquired by applying the Laplace transform to Eqs. (9)–(11). The $T_{\mathrm{w}}(t,\xi)$ is described as follows:

$$T_{\mathrm{w}}(t,\xi) = \frac{Ah^*}{\sqrt{\left(h^* + \sqrt{\omega/2a}\right)^2 + \left(\sqrt{\omega/2a}\right)^2}} \times \exp\left(-\sqrt{\omega/2a}\cdot\xi\right)\sin\left(\omega t + \varphi - \sqrt{\omega/2a}\cdot\xi - \varepsilon\right), \tag{12}$$

here,

$$h^* = h/\lambda, \tag{13}$$

$$\varepsilon = \tan^{-1}\left[\sqrt{\omega/2a}\Big/\left(h^* + \sqrt{\omega/2a}\right)\right]. \tag{14}$$

As discussed before, h was assumed to be constant in time. Namely, the each frequency component is independent of the rest of frequency components and random wave can be expressed as linear combinations of every frequency components. Then, the power and phase of transfer function can be described as follows:

$$\begin{aligned}&\text{Power}: \left[\frac{h^*}{\sqrt{\left(h^* + \sqrt{\omega/2a}\right)^2 + \left(\sqrt{\omega/2a}\right)^2}} \exp\left(-\sqrt{\omega/2a}\cdot\xi\right)\right]^2.\\ &\text{Phase}: \sqrt{\omega/2a}\cdot\xi + \tan^{-1}\left[\sqrt{\omega/2a}/\left(h^* + \sqrt{\omega/2a}\right)\right]\end{aligned} \tag{15}$$

Here, the transfer functions of temperature fluctuation between the fluid and the wall were obtained based on both the experimental data and the theory. Thus, the heat transfer coefficient, h, used in the theory can be estimated so as to fit the theoretical curve of the power to the experimental data. Then the theoretical curve of the phase delay can be determined by using the estimated value of h.

In Fig. 10, the solid line for the power shows the fitting result of Eq. (15) applied to the experimental data. The solid line for the phase shows the theoretical curve based on Eq. (15) and the obtained heat transfer coefficients. The fitting line for the power was close to the experimental results up until ~10 Hz. The function of Eq. (15), in which the heat transfer coefficient was constant in time and frequency, was suitable. In the isovelocity case, the phase was scattered. It might be due to a slight deviance of frequency components at the averaging process of spectrum for the transfer function. In the non-isovelocity case, however, the phase in the transfer function was in agreement with the theoretical equation, Eq. (15).

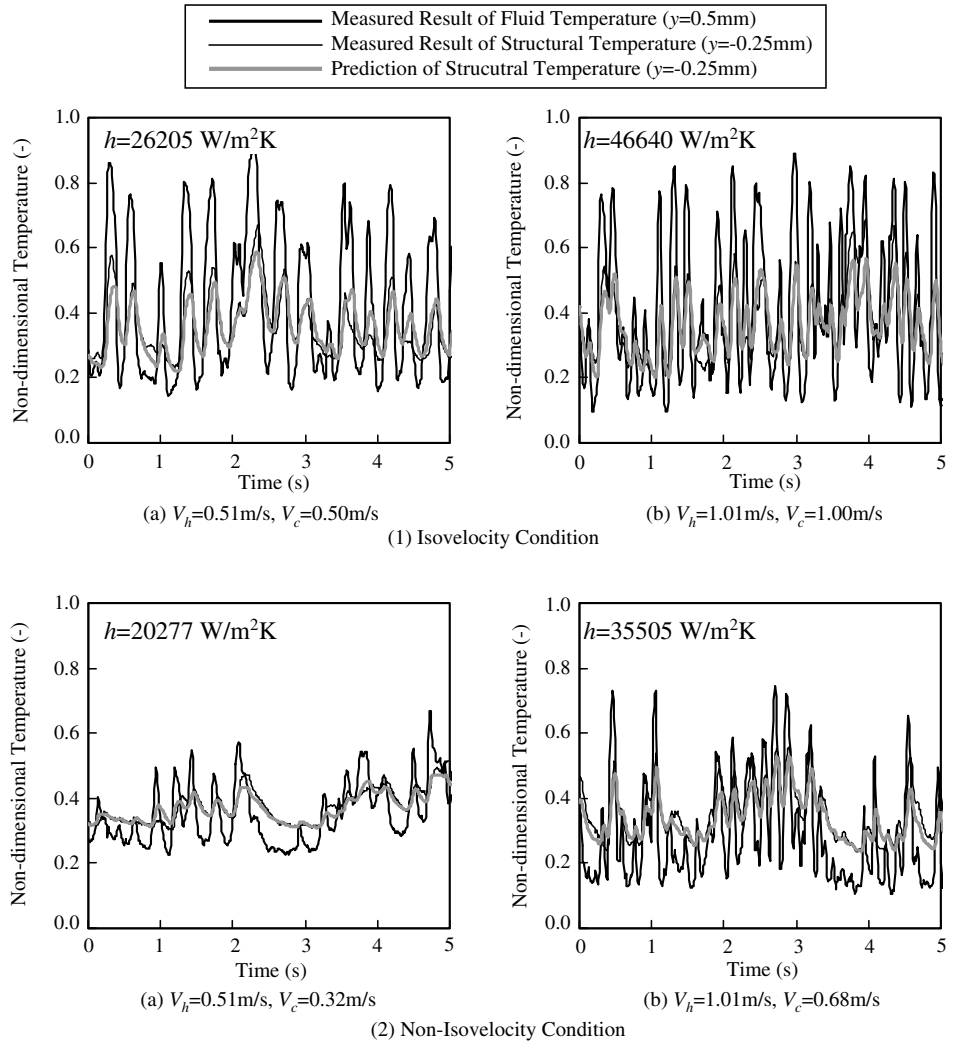

Fig. 11. Comparison of temperature histories at $y = -0.25$ mm (in the structure) between the experiment and the prediction from measured temperature in fluid ($y = 0.5$ mm) using Eqs. (4) and (14).

In these discussions of heat transfer and heat conduction, one-dimensional equations were used. The flow field of parallel jets was three-dimensional. The scale of flow and vortex will have a size of the jet outlet, that is order of 10 mm. However, the measured positions in the fluid and wall are in range of 0.5 mm. Then one-dimensional equations can represent the transfer functions of experimental data in depth direction of the wall as shown in Figs. 6 and 10. This means that one-dimensional heat transfer is appropriate to see the fluid and wall temperatures near the wall surface.

In order to confirm that the constant heat transfer coefficient was enough to represent the transfer characteristics of temperature fluctuation, the wall temperature was predicted by using h from the fluid temperature. Fig. 11 shows the comparison of temperature histories at $y = -0.25$ mm (in the structure) between the experiment and the prediction based on the measured temperature in fluid ($y = 0.5$ mm). The prediction was made as follows; (1) the fluid temperature at $y = 0.5$ mm was converted into frequency domain by the FFT, (2) the frequency components of temperature fluctuation in the wall ($y = -0.25$ mm) were acquired by applying Eq. (15) and the obtained heat transfer coefficient to frequency data of the fluid temperature at $y = 0.5$ mm, (3) the time history of temperature at $y = -0.25$ mm was obtained by the inverse FFT from the temperature in frequency domain.

The predicted temperature trends in the wall were in good agreements with the experimental results. It means that the constant heat transfer coefficient, h, is enough to describe the non-stationary heat transfer phenomena from the fluid to the structure. Then large decay of amplitude from fluid temperature to wall temperature can be predicted by using the h. The obtained heat transfer coefficient could be used to estimate the Biot number for the frequency response function and then the thermal stress in the wall.

Fig. 12 shows the relationship between the obtained heat transfer coefficient and Peclet number in our wall jet geometry. The Peclet number was calculated by using the hydraulic length defined as two times of a distance between two plates ($D_e = 0.36$ m) and the discharged velocity in the cold jet. The heat transfer was estimated at $x = -15$ mm and $z = 100$ mm. This point was close to the cold jet position and we considered that the cold jet velocity was adequate for the definition of Peclet number. The heat transfer coefficients were increased as Peclet number increased independent on the discharged velocity ratio. Poppendiek [22] showed the heat transfer characteristics in a short duct for liquid metal as follows:

$$Nu_{D_e} = 0.638\left(\frac{Pe \cdot D}{x}\right)^{7/15}, \tag{16}$$

here, x was a running length, which was defined as the distance from the nozzle exit in this study ($x = 0.1$ m).

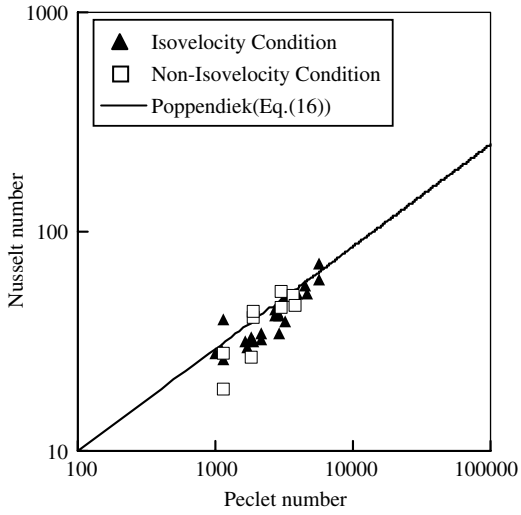

Fig. 12. Relationship between the obtained heat transfer coefficient and Peclet number in our wall jet geometry.

Peclet number dependency of the obtained heat transfer coefficient was in good agreement with Eq. (16). Consequently, we could show that the non-stationary heat transfer characteristics were close to the stationary heat transfer characteristics for the dependency of Peclet number.

4. Conclusions

In order to evaluate thermal striping phenomena for sodium cooled fast reactors, we performed a sodium experiment in which triple parallel jets flowed along the stainless steel wall (wall jet geometry). Temperatures were measured in the fluid and the structure by thermocouples to investigate the transfer of temperature fluctuation. Following findings were obtained.

The area of high fluctuation intensity region became small at the neighborhood of the wall surface. he contours of time-averaged temperature and fluctuation intensity in the higher discharged velocity case were similar to those in the lower discharged velocity case.

The amplitude of temperature fluctuation was severely attenuated in the process of the transfer from the fluid to the wall. The consideration of the attenuation make it possible to evaluate the thermal stress legitimately.

A heat transfer coefficient, h, was assumed to be constant in time in order to apply to simple design method of thermal striping. An evaluation method of h was developed, where the transfer function of the temperature fluctuation between the fluid and wall was used. The obtained h was sufficient to predict the temperature fluctuation in the wall from the fluid temperature.

The heat transfer coefficients were obtained as a function of Peclet number based on the discharged velocity in this wall jet geometry. The coefficients were independent of the discharged velocity profile (isovelocity or non-isovelocity). The coefficients depended on the 7/15th power of Peclet number.

Acknowledgements

The authors appreciate Prof. Madarame of University of Tokyo for his encouragement. And also, the authors are grateful to Dr. Moriya of Central Research Institute of Electric Power Industry, Dr. Kasahara of Japan Atomic Energy Agency for their advices.

References

[1] D.S. Wood, Proposal for design against thermal striping, Nucl. Energy 6 (1980) 433–437.
[2] J.E. Brunings, LMFBR thermal-striping evaluation, Interim report, Research Project 1704-11, prepared by Rockwell International Energy Systems Group (1982), EPRI-NP-2672.
[3] C. Betts, C. Bourman, N. Sheriff, Thermal striping in liquid metal cooled fast breeder reactors, in: Proceedings of the Second International Topical Meeting on Nuclear Reactor Thermal–Hydraulics, Santa Barbara, CA, vol. 2, 1983, pp. 1292–1301.
[4] S. Moriya, S. Ushijima, N. Tanaka, S. Adachi, I. Ohshima, Prediction of thermal striping in reactors, in: International Conference of Fast Reactors and Related Fuel Cycles, Kyoto, Japan, vol. 1, 1991, pp. 10.6.1–10.6.10.
[5] T. Muramatsu, Development of thermohydraulics computer programs for thermal striping phenomena, in: Specialists meeting on correlation between material properties and thermohydraulics conditions in LMFRs, Aix-en-Provence, France, 1994, IWGFR/90.
[6] A. Tokuhiro, N. Kimura, J. Kobayashi, H. Miyakoshi, An investigation on convective mixing of two buoyant, quasi-planar jets with a non-buoyant jet in-between by ultrasound Doppler velocimetry, in: Proceedings of 6th International Conference on Nuclear Engineering, San Diego, CA, 1998, ICONE-6058.
[7] D. Tenchine, H.Y. Nam, Thermal hydraulics of co-axial sodium jets, Am. Inst. Chem. Eng. Symp. Ser. 83 257 (1987) 151–156.
[8] D. Tenchine, J.P. Moro, Experimental and numerical study of coaxial jets, in: Proceedings of Eighth International Topical Meeting on Nuclear Reactor Thermal-Hydraulics, Kyoto, Japan, vol. 3, 1997, pp. 1381–1387.
[9] A. Tokuhiro, N. Kimura, H. Miyakoshi, An experimental investigation on thermal striping. Part I: Mixing of a vertical jet with two buoyant heated jets as measured by ultrasound Doppler velocimetry, in: Proceedings of Eighth International Topical Meeting on Nuclear Reactor Thermal-Hydraulics, Kyoto, Japan, vol. 3, 1997, pp. 1712–1723.
[10] A. Tokuhiro, N. Kimura, An experimental investigation on thermal striping. Mixing phenomena of a vertical non-buoyant jet with two adjacent buoyant jets as measured by ultrasound Doppler velocimetry, Nucl. Eng. Des. 188 (1999) 49–73.
[11] N. Kimura, A. Tokuhiro, H. Miyakoshi, An experimental investigation on thermal striping. Part II: Heat transfer and temperature measurement results, in: Proceedings of Eighth International Topical Meeting on Nuclear Reactor Thermal-Hydraulics, Kyoto, Japan, vol. 3, 1997, pp. 1724–1734.
[12] N. Kimura, M. Nishimura, H. Kamide, Study on convective mixing for thermal striping phenomena (experimental analyses on mixing process in parallel triple-jet and comparisons between numerical methods), JSME Int. J. Ser. B 45 (3) (2002) 592–599.
[13] M. Igarashi, M. Tanaka, S. Kawashima, H. Kamide, Experimental study on fluid mixing for evaluation of thermal striping in T-pipe junction, in: Proceedings of 10th International Conference on Nuclear Engineering, Washington DC, 2002, ICONE10-22255.
[14] M. Igarashi, M. Tanaka, N. Kimura, H. Kamide, Study o fluid mixing phenomena fro evaluation of thermal striping in a mixing tee, in: Proceedings of 10th International Topical Meeting on Nucelar Reactor Thermal-Hydraulics, Seoul, Korea, 2003, A00512.
[15] T. Muramatsu, Numerical analysis of nonstationary thermal response characteristics for a fluid-structure interaction system, J. Press. Vess. Technol. 121 (1999) 1381–1387.
[16] Xue-Ren. Wu, A. Janne Carlsson, Weight Functions and Stress Intensity Factor Solutions, Elsevier Science Ltd., Pergamon, 1992.
[17] N. Kasahara, A. Yacumpai, H. Takasho, Structural response diagram approach for evaluation of thermal striping phenomena, in: Proceedings of 15th International Conference on Structural Mechanics in Reactor Technology, Seoul, Korea, vol. IV, 1999, pp. 201–208.
[18] N. Kasahara, H. Takasho, Stress response functions to multi-dimensional spatial fluctuations of fluid temperature, in: Proceedings of 2002 Pressure Vessels and Piping Conference, Vancouver, Canada, 2002, 1327, pp. 25–32.
[19] H. Choe, C.M. Kwong, Turbulent Temperature Fluctuation and Heat Transfer to a Metal Surface Resulting from the Mixing of Cold and Hot Water, American Society of Mechanical Engineers Publication, 1979, 79-WA-HT-23.
[20] N. Kimura, M. Igarashi, H. Kamide, Investigation on convective mixing of triple-jet -evaluation of turbulent quantities using particle image velocimetry and direct numerical simulation, in: Proceedings of Eighth International Symposium on Flow Modeling and Turbulence Measurements, Tokyo, Japan, 2001, pp. 651–658.
[21] N. Kasahara, N. Kimura, H. Kamide, Thermal fatigue evaluation method based on power spectrum density functions against fluid temperature fluctuation, in: Proceedings of 2005 Pressure Vessels and Piping Conference, Denver, CO, 2005, PVP2005–71307.
[22] H. F. Poppendiek, Forced convection heat transfer in thermal entrance regions, Part. I. Rept. No. ORNL-913, Oak Rigde National Laboratory, 1952.